PROTEINS: Structure, Function, and Genetics 25:366–378 (1996)

The Influence of a Protein on Water Dynamics in Its Vicinity Investigated by Molecular Dynamics Simulation

Roger Abseher, Hellfried Schreiber, and Othmar Steinhauser
Institut für Theoretische Chemie, Universität Wien, A-1090 Vienna, Austria

ABSTRACT **A system containing the globular protein ubiquitin and 4,197 water molecules has been used for the analysis of the influence exerted by a protein on solvent dynamics in its vicinity. Using Voronoi polyhedra, the solvent has been divided into three subsets, i.e., the first and second hydration shell, and the remaining bulk, which is hardly affected by the protein. Translational motion in the first shell is retarded by a factor of 3 in comparison to bulk. Several molecules in the first shell do not reach the diffusive regime within 100 ps. Shell-averaged orientational autocorrelation functions, which are also subject to a retardation effect, cannot be modeled by a single exponential time law, but are instead well-described by a Kohlrausch-Williams-Watts (KWW) function. The underlying distribution of single-molecule rotational correlation times is both obtained directly from the simulation and derived theoretically. The temperature dependence of reorientation is characterized by a strongly varying correlation time, but a virtually temperature-independent KWW exponent. Thus, the coupling of water structure relaxation with the respective environment, which is characteristic of each solvation shell, is hardly affected by temperature. In other words, the functional form of the distributions of single-molecule rotational correlation times is not subject to a temperature effect. On average, a correlation between reorientation and lifetimes of neighborhood relations is observed.**

Key words: hydration/solvation, Kohlrausch-Williams-Watts relaxation, diffusion, residence time, Voronoi polyhedra, ubiquitin

INTRODUCTION

Since the structure determination of biological macromolecules has been well-established, it is now the solvent in the proximity of a macromolecular solute that increasingly receives attention.[1–3] In parallel, molecular dynamics simulations of an explicit solvent environment have become common practice,[4,5] which, besides providing a realistic description of protein dynamics, allow the investigation of the influence that protein and water exert on each other. There are two types of water directly interacting with a protein, i.e., surface water and, if present, internal water. Structure and dynamics of water close to a protein can be observed by a variety of experimental methods. Neutron and X-ray diffraction yield time-averaged positions of "hydration sites," i.e., sites which are preferably occupied by a water molecule in the crystal. These sites are not equivalent to a longtime residence of a single molecule, but come about by averaging over a dynamic exchange. Spectroscopic methods allow an estimate of the time scale of the dynamic processes in the protein-solvent interface. The combined use of laboratory frame and rotating frame nuclear Overhauser effect (NOE and ROE, respectively) techniques[6] permits the distinction between fast- and slow-exchanging hydration water molecules. A direct nuclear magnetic resonance (NMR) observation of a retardation effect of a solute on water dynamics has recently been reported.[7] Dielectric spectroscopy revealed nonfreezing water on the surface of albumin.[8] Nonfreezing water is influenced by the protein so strongly that it is unable to adopt an ice structure. Data obtained with these methods are complemented by sorption thermodynamic measurements. Microcalorimetric determination of the specific heat of a protein solution as a function of the fraction of water allows an estimate of the number of water molecules influenced by the protein.[9] Another approach which is capable of providing high spatial and time resolution is computer simulation.[10–15]

Both structure and dynamics of the solvating water molecules are affected by the presence of a protein. For the analysis of these effects the protein can be considered in two ways. As the protein displays on its surface a variety of functional groups with differing physicochemical properties, protein hydration can be studied on a full-detail level accounting for local differences in the mutual influence of solute

Received September 19, 1995; revision accepted December 12, 1995.
Address reprint requests to Hellfried Schreiber, Institut für Theoretische Chemie, Universität Wien, Währinger Strasse 17, A-1090 Vienna, Austria.

and solvent. Alternatively, the protein can be considered as a whole, and solvent properties can be monitored in a spatially averaged manner, i.e., as a function of the distance from the protein surface or of the solvation shell number. The spatially averaged structure of the protein-solvent interface is quantified by the perpendicular distribution function.[16] Zooming in and inspecting local deviations from the water bulk density,[17] a fractal density measure has been used for the characterization of the solute-solvent interface.[18]

In this paper we report on a molecular dynamics simulation study of the water dynamics in the vicinity of the small globular protein ubiquitin.[19] The Voronoi polyhedra concept[20,21] has been employed for the definition of hydration shells around ubiquitin. Ubiquitin contains no internal water molecules.[19,22] Proton spin-lattice relaxation observed by NMR may be decomposed into an intermolecular and an intramolecular component. On the level of molecular motion this corresponds to translation and reorientation. On average we observe a decreased translational and rotational mobility near the protein. A fractal time behavior is detected for orientational autocorrelation functions and residence correlation functions. The temperature dependence of the fractal time behavior has been investigated within a physiologically relevant temperature interval.

The occurrence of fractal time is characteristic of "glassy" relaxation in strongly interacting systems.[23,24] In such systems the unperturbed relaxation mode of the primitive species, e.g., a solvent molecule, couples with the complex dynamics of the environment, e.g., the surface of the macromolecule. The distribution of relaxation times of individual solvent molecules broadens, and typically long-tail distributions are observed. Longer relaxation times occurring with lower probabilities yield a fractal time dependence upon averaging over individual solvent molecules.

METHODS

Molecular Dynamics Calculations

The simulated system consists of the small globular protein ubiquitin,[19] eight counterions, and 4,197 simple point change (SPC)[25] water molecules. This is equivalent to a total of 13,345 atoms which occupy a volume of $5.0 \times 5.0 \times 5.5$ nm^3 at 300 K. Structural and dynamic properties of SPC water have been extensively surveyed.[26] The initial structure of ubiquitin has been taken from the Brookhaven data bank (entry *1ubq.pdb*). The molecular topology has been generated with the program PROGMT of the GROMOS86 package.[27] The interaction function parameters are those of the 37C4 united atom force field.

The simulations were carried out with a program package consisting of self-written code, but using the GROMOS topology and force field. Thereby, special emphasis was laid upon the correct treatment of electrostatic interactions by the Ewald method.[28–30] Volume, temperature,[31] particle number, and bond lengths[32] were kept constant during a simulation. The time step was 2 fs and the neighbor-lists were updated every 10 time steps.

Simulations at 273 K, 300 K, and 350 K were performed. For the simulation at 350 K, the simulation box was expanded from $5.0 \times 5.0 \times 5.5$ nm^3 to $5.04 \times 5.04 \times 5.54$ nm^3. This accounts for the change of density of pure water[33] from 0.9965 g cm^{-3} at 300 K to 0.9736 g cm^{-3} at 350 K. Analogously, the box was contracted from $5.0 \times 5.0 \times 5.5$ nm^3 to $4.9944 \times 4.9944 \times 5.49384$ nm^3 for the simulation at 273 K. The density of pure water at 273 K is 0.9998 g cm^{-3}. The coordinates of the water molecules of a 300 K frame were scaled with the same factor in order to make them fit into the slightly smaller box. After setting up the systems for the simulations at 273 and 350 K, they were equilibrated for 20 and 30 ps, respectively. As the velocity autocorrelation functions and the reorientational correlation functions decay at different time scales, different sampling intervals and trajectory lengths become necessary. For monitoring velocity autocorrelation functions and the short-time behavior of reorientational correlation functions, trajectories of 10-ps length were sufficient. Coordinate frames were written in intervals of 0.02 psec. For observation of the complete decay of orientational autocorrelation functions, a time window of approximately 30 ps is necessary. Simulations of 750 ps (300 K) and 110 ps (273 K, 350 K) length, with 1 ps and 0.5 ps sampling intervals, respectively, were performed for this purpose.

The simulations were performed on local HP9000/720 and SGI Indy workstations and on a DEC-α workstation cluster at the Computer Center of the University of Vienna.

Voronoi Polyhedra

For the analysis of protein hydration, the concept of the solvation shell is useful. The definition of a solvation shell may follow two different paradigms. One approach makes use of the radial pair distribution function of water oxygen atoms about the atom types that occur on the surface of the protein. On the basis of pair distribution functions, cutoff radii are chosen that define the limit of a solvation shell.[12] In other words, this method introduces a set of atom type-specific parameters. Furthermore, this approach does not take into account instantaneous fluctuations in the configuration of the water molecules around a surface atom of the solute.

Alternatively, the instantaneous positions of the solvent molecules are used for the determination of the solvation shell. This holds for the Voronoi polyhedra method.[20,34] The construction of the polyhedra is a geometrical procedure and does not make

use of any parameter. The Voronoi method is used either for the calculation of atomic volumes[21,35] or for the determination of the nearest neighbors of an atom.[36] For constructing the solvation shell around an atom P_S on the surface of the protein, a plane orthogonal on the vector $\overrightarrow{P_S OW_i}$ is erected in all water oxygens OW_i (for the calculation of the volume of P_S this plane would be erected between P_S and OW_i, i.e., midway between the two atoms). A water molecule with oxygen OW_j is rejected as a member of the first shell around P_S if P_S and OW_j lie on different sides of at least one of the planes erected. The planes erected at the positions of the remaining oxygen atoms form a (usually irregular) polyhedron making up the first hydration shell around P_S. The second hydration shell is determined by considering the water molecules of the first shell as the solute. This procedure generates three subsets of solvent, i.e., the first and second solvation shell, and the rest, referred to as "bulk" in the following. The latter subset is expected to be influenced in a negligible way by the protein.[14,37]

For economical reasons, out of all protein atoms $\{P\}$ a subset of potentially solvated atoms $\{P_s\}$ with nonvanishing solvent-accessible surface[38] is determined for each coordinate frame. In order to reduce the number of atoms to be handled, a subset of all water molecules is chosen, too. This is done by determining a layer of 0.65-nm thickness around the respective solute.

Structure of the Protein-Water Interface

For the analysis of the protein–water interface in terms of the protein as a single entire solute, the perpendicular distribution function $g\perp(r)$ was introduced.[16] For each water oxygen only the distance to the closest atom on the protein surface is considered. Here the contribution of the first shell to the perpendicular distribution function is inspected.

$$P_\perp^1(r) = \left(1/\sum_{t=0}^{T} N_W^1(t)\right) \cdot \sum_{t=0}^{T} \sum_{i=1}^{N_W^1(t)} \delta(\mathrm{Inf}[|\vec{r}_p(t) - \vec{r}_{ow,i}(t)|]_{P=1,N_p} - r) \quad (1)$$

This is a normalized probability P for the occurrence of a distance r between the oxygen OW_i of a first-shell water molecule and the closest protein atom P. T is the trajectory length, i.e., the number of coordinate frames. N_P and $N_W^1(t)$ are the number of protein atoms and the number of first-shell water molecules for a given coordinate frame, respectively.

Dynamical Properties

The dynamical properties of water in the solvated ubiquitin system were determined for whole solvation shells, i.e., first and second shell around the protein and the remaining bulk. We calculated shell-averaged autocorrelation functions which are determined by averaging over those single-molecule correlation functions which are pertinent to the respective shells. Thus, the relaxation of an average "particle" is investigated, which is not to be confused with the time behavior of collective properties. During the trajectory it frequently happens that a water molecule leaves the shell of which it has been a member so far and joins another shell. In this case this molecule begins a "new life" in the new shell and gives rise to new single-molecule autocorrelation functions. If remigration to the previously occupied shell occurs, the water molecule is again considered as a new individual, which seems reasonable, as after remigration to, for instance, the first shell, a water molecule may occupy a different hydration site on the surface of the protein. Thus, with growing trajectory length the total number of single-molecule correlation functions exceeds by far the total number of water molecules in the system. The general method for the calculation of shell-averaged time-dependent properties $CF^{\#}(t)$ from the single-molecule properties $CF_i^{\#}(t)$ is as follows (superscript # indicates shell number):

$$CF^{\#}(t) = (1/N_{CF}^{\#}(t)) \cdot \sum_{i=1}^{N_{CF}^{\#}(t)} CF_i^{\#}(t) \quad (2)$$

Owing to the limited residence time of water molecules within a given shell, the number of correlation functions $N_{CF}^{\#}$ defined up to a time t is a function of t. As there is a continuous exchange of molecules between the hydration shells, an upper limit for the residence time within a shell is observed. This time $t_{max}^{\#}$ imposes an upper bound for the time window of time-dependent properties. For $t > t_{max}^{\#}$ the number of correlation functions $N_{CF}^{\#}(t)$ is zero.

The average translational motion is monitored by the autocorrelation function of the velocity of the center-of-mass

$$VACF(t) = \overline{\vec{v}(0)\cdot\vec{v}(t)}/\overline{\vec{v}(0)\cdot\vec{v}(0)} \quad (3)$$

and by the mean-square displacement of the center-of-mass

$$MSD(t) = \overline{(\vec{r}(t) - \vec{r}(0))^2}. \quad (4)$$

For $t \to \infty$, MSD(t) displays a linear time dependence

$$\overline{(\vec{r}(t) - \vec{r}(0))^2} = 6D \cdot t \quad (5)$$

with D, the translational diffusion coefficient. Closer inspection of the short-time behavior reveals a nonvanishing ordinate intercept d for the extrapolation of the linear expression 5 for $t \to 0$.

$$\overline{(\vec{r}(t) - \vec{r}(0))^2} = \underbrace{2\int_o^t \overline{\vec{v}(0)\vec{v}(\tau)}d\tau \cdot t}_{3D} - \underbrace{2\int_o^t \tau\cdot\overline{\vec{v}(0)\vec{v}(\tau)}d\tau}_{d} \quad (6)$$

The sign of the ordinate intercept may be either negative or positive, depending on the strength of the intermolecular interaction.

Reorientation is described by the Legendre polynomials $P_l(\cos\theta(t))$, where $\theta(t)$ is the angle between a molecule-fixed vector at two different times $\tau = 0$ and $\tau = t$.

$$P_1(t) = \overline{\cos\theta(t)} \quad (7)$$

$$P_2(t) = (3/2)\overline{(\cos^2\theta(t) - 1)} \quad (8)$$

Different experimental methods are sensitive to the motion of different vectors. The first Legendre polynomial of the dipole moment $\vec{\mu}$ of the water molecule is the essential quantity of infrared spectroscopy. NMR measurements sample the second-order reorientation of the intramolecular proton-proton vector (proton spin-lattice relaxation) or the OH-vector (deuteron quadrupolar relaxation).

For the investigation of migration processes between hydration shells, the residence correlation function[14,36] was used:

$$\mathrm{RCF}(t) = \overline{\chi(0)\chi(t)}/\overline{\chi(0)^2}. \quad (9)$$

$\chi(t)$ is a Boolean variable. Its value depends on the water molecule being a member of a hydration shell at time t or not. The decay of RCF(t) displays the lifetime of neighborhood relation, i.e., the probability of encountering a particle within the same shell after time t. Alternatively, a residence time distribution, i.e., a probability distribution of residence times within a shell, was determined.

RESULTS

Structure of the Protein-Water Interface

The probability function $P_\perp^1(r)$ (cf. Methods) shows the distribution of distances between first-shell water oxygens and the respective closest atoms on the protein surface. A 750-psec average (sampling interval, 1 psec) at 300 K is shown in Figure 1.

$P_\perp^1(r)$ displays peaks at the hydrogen bond distance and the distance for contact between water oxygen and heavy atoms (C, N, O, S) on the protein surface. Furthermore, $P_\perp^1(r)$ monitors how far away from the protein surface a member of the first hydration shell may be encountered. As the Voronoi approach is sensitive to short-time fluctuations in the structure of the hydration shell, it may result in maximal protein–water distances for the instantaneous hydration shells that differ significantly from the values obtained from the equilibrium pair distribution function. As a consequence, there is a non-negligible number of water molecules that are part of the first layer of solvent around the protein according to the Voronoi definition but that are not caught by the cutoff approach. On the other hand, a water molecule within the cutoff may be excluded by the Voronoi method if the adjacent molecules form a suitable polyeder. Such a molecule appears as a member of the second shell according to the Voronoi method. In order to illustrate this quantitatively we compared the two approaches for a single coordinate frame. The Voronoi method determines 570 first-shell molecules, and the cutoff method using the atom type-specific parameters[12] determines 510. Five hundred and five molecules occur in both sets: 65 are caught by the Voronoi method, and only five by the cutoff method.

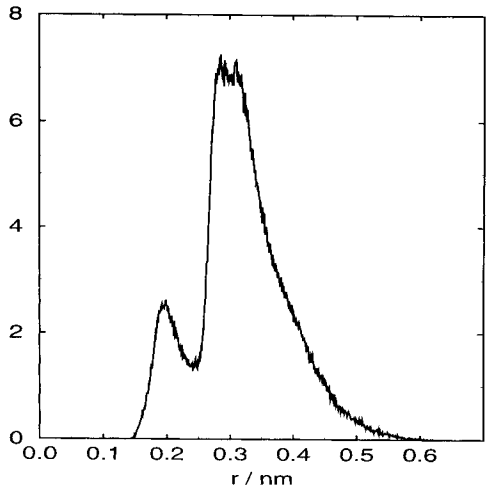

Fig. 1. Distribution of distances between first-shell water oxygens and protein surface atoms. For each water oxygen, only the distance to the closest protein surface is considered. The first peak at 0.195 nm stems from waters making hydrogen bridges to polar hydrogens on the protein surface. Contact between water and surface heavy atoms gives rise to the second peak, centered around 0.30 nm. First-shell waters may occur at distances up to 0.6 nm from the closest protein atom.

The distributions of occupation numbers, i.e., the number of water molecules in the first and second hydration shells around the ubiquitin, are given in Figure 2. The Voronoi approach yields an average hydration level h (g water/g protein) of 1.15 for a system containing protein and first shell. Applying the cutoff approach[12] to ubiquitin, values of $h > 1.0$ are obtained as well (data not shown).

Time Correlation Functions

Translational motion

The shell-averaged velocity autocorrelation functions at 300 K are shown in Figure 3a. At first sight, there are only slight changes in the velocity autocorrelation function when moving from bulk to the second and first hydration shells. Approaching the protein, the correlation function is shifted throughout to more negative values. For comparison, Lee and Rossky[14] found an increase in depth of the first minimum of the velocity autocorrelation function of the first layer of water on a polar model surface, but a decrease in depth for a nonpolar surface. Thus, the effect of polar residues dominates in the case of ubi-

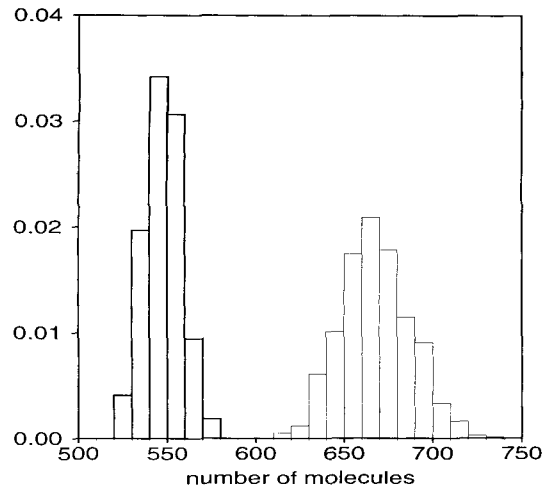

Fig. 2. Normalized distributions of occupation numbers of the first (thick lines) and second (thin lines) hydration shell, obtained by Voronoi method from a 750-ps trajectory (sampling interval, 1 ps) at 300 K. Average numbers of water molecules are 547.3 (first shell) and 667.5 (second shell); 547.3 water molecules are equivalent to a hydration level h (g water/g protein) of 1.15.

quitin. The power spectra obtained by Fourier transformation of the velocity autocorrelation functions did not reveal additional modes for the first hydration shell (Fig. 3b). Thus, the velocity autocorrelation functions differ only quantitatively.

As the diffusion coefficient is given by the integral of the velocity autocorrelation function (cf. Eq. 6), slight changes in the correlation function exert a significant influence on the mean square displacements of the centers-of-mass. The mean-square displacements were recorded separately from the 750-ps trajectory. The data for 300 K are shown in Figure 4.

On average, translational motion is retarded in the vicinity of the protein. The translational diffusion coefficient D is related to the slope of the plots MSD(t) vs. t by Eq. 5. Data are given in Table I. The sign of the NOEs between water and hydrogens on the protein surface depends on the diffusion coefficient of the water molecules involved.[6] As generally positive NOEs are observed, the motion of the first-shell waters is still fast in comparison to the overall tumbling of the protein. Experimental data for the bovine pancreatic trypsin inhibitor (BPTI) at 279 K[6] have been modeled by assuming a retardation factor of less than 4 for translational motion of single molecules in the first shell. From the simulation data at 300 K, we find a quotient of shell-averaged diffusion coefficients D (bulk)/D (first shell) of 3.3 (cf. Table I).

For the bulk, the diffusional regime is reached within 1 ps. For the solvent perturbed by the protein this occurs much later, if at all. This is due to the heterogeneity of local environments in the vicinity of the protein, which gives rise to a diversity of motional rates. In the first shell, even for single molecules the diffusional regime is not reached within 100 ps. In Figure 5 the mean-square displacements of a single arbitrary first-shell water molecule and a bulk water molecule are compared. Both molecules are permanent in the sense that they stay within the same water subset throughout the simulation, e.g., for 750 ps. Single molecules in the bulk do not deviate very much from the average, whereas first-shell waters do.

An analysis of the self-diffusion coefficient of water under the influence of a protein was performed at a high spatial resolution by Lounnas et al.[11] Instead of tracing individual molecules for their entire residence time within a shell, they determined the average diffusion coefficient within a sphere of 1 Å radius around a point on a grid. Thus, "site" properties are observed, which differ from single-molecule properties.

Reorientation

The time behavior of a molecule-fixed vector has been used for the determination of the first and second Legendre polynomials (P_1, P_2) as a function of time (cf. Methods). The vectors considered are the molecular dipole moment $\vec{\mu}$, the intramolecular HH vector, and the OH bond vector. On average, the protein exerts a retardation effect on water reorientation in its vicinity. This effect is pronounced for the first hydration shell and weak for the second shell (Fig. 6). The behavior of the three vectors splits up, especially within the first hydration shell. The vector pointing along the dipole moment is the most rigid one. This finding suggests that in configurations where the dipole moment is locked owing to interactions with the protein surface and/or other water molecules, the HH vector is still free to rotate. The OH bond vector is just a linear combination of these two.

For a quantitative description of the effects exerted on water reorientation by the protein, the direction of the vector considered, and the temperature, fits of the correlation functions have been performed. Depending on the time scale, data in the interval [0, 10 ps] or [0, 20 ps] have been used for fitting. It turns out that the shell-averaged orientational autocorrelation functions do not follow simple exponential characteristics. Instead, stretched exponentials as target functions yield an excellent description of the curves using two parameters:

$$g(t) = \exp(-(t/\tau_\kappa)^\beta). \qquad (10)$$

This type of time behavior, termed Kohlrausch-Williams-Watts (KWW) relaxation,[39,40] involves in addition to a relaxation time τ_κ a fractal exponent β. This introduces the concept of "fractal time" which is inherent to numerous phenomena in condensed matter physics.[24] In a bilogarithmic plot of $-\ln P_2(t)$ vs. t the parameter β can be read directly (Fig. 7).

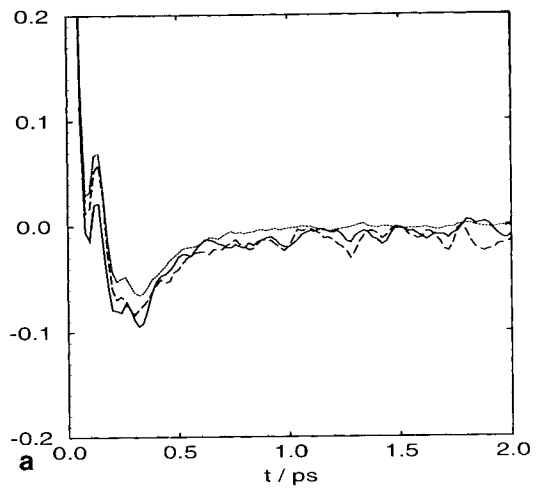

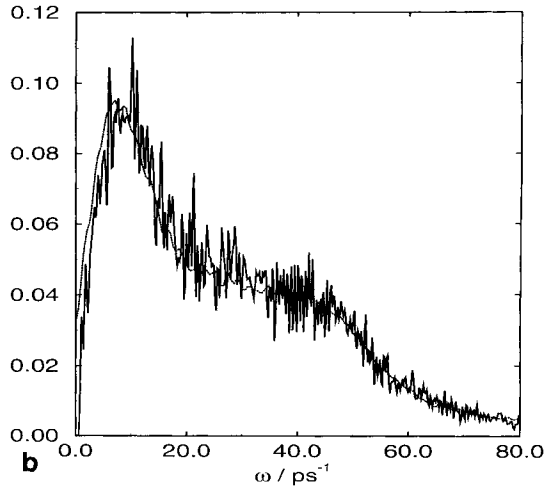

Fig. 3. **a:** Center-of-mass velocity autocorrelation functions at 300 K. Each curve represents an average over water molecules occupying a solvation shell around ubiquitin: first shell (continuous line), second shell (broken line), and bulk (dotted line). **b:** Power spectra obtained by Fourier transformation of shell-averaged velocity autocorrelation functions for the first shell (continuous line) and bulk (dotted line) at 300 K.

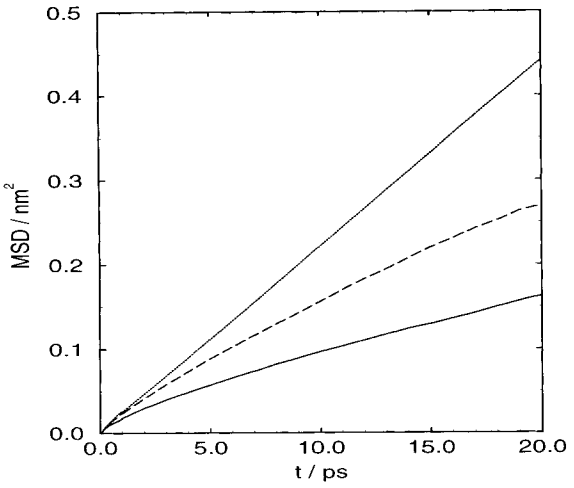

Fig. 4. Shell-averaged mean-square displacements of centers-of-mass (300 K). Continuous line, first shell; dashed line, second shell; dotted line, bulk.

TABLE I. Average Self-Diffusion Coefficient of Water Around Ubiquitin at 300 K*

	D/m^2s^{-1}	ξ_D
First shell	1.10×10^{-9}	3.35
Second shell	1.89×10^{-9}	1.95
Bulk	3.68×10^{-9}	1.00

*Values are obtained from the slope of the MSD plots in the interval from 10–20 psec. The bulk fraction (water beyond the second shell) has the same self-diffusion coefficient as pure SPC water at 300 K.[26] In the third column, retardation factors $\xi_D = D(\text{bulk})/D$ are given.

We used the Levenberg-Marquardt least-squares fit procedure[41] for the determination of τ_κ and β. Data for the shell-averaged first and second Legendre polynomials of the three molecule-fixed vectors considered are given in Table II.

The protein has a significant effect on the value of the KWW exponent β. Considering $P_2(t)$, β shifts from a value of approximately 0.75 for the bulk fraction to 0.50 for the first hydration shell. Thus, the deviation from a simple exponential time behavior increases in the vicinity of the protein. However, even for the bulk, β differs significantly from 1.0. A 200-ps control simulation of pure SPC water at 300 K yields values of β between 0.71–0.73, depending on the vector considered (data not shown). The relaxation of bulk water appears to be a borderline case. It may still be interpreted in terms of single exponential Debye relaxation,[26] although our bulk data are better modeled by a stretched exponential (Fig. 8). For the first shell the single exponential model completely breaks down. Interestingly, a value of $\beta = 0.50$ is equivalent to a dependence of the P_2 reorientation on the square root of time: $P_2(t) = \exp(-\sqrt{t/\tau_\kappa})$. A simulation of a system very simple in comparison to the solvated ubiquitin system yielded a similar result. The average $P_2(t)$ of the first shell of Stockmayer particles around a spherical solute particle with a large dipole moment shows a β of approximately 0.5.[36]

Deviations from an exponential time law may be interpreted as a result of relaxation time distributions.[42,43] Therefore, the single-molecule correlation functions, which upon averaging give rise to the stretched exponential correlation functions considered so far, have been inspected. The single-molecule P_2 correlation functions display the following behavior, which is basically familiar from simula-

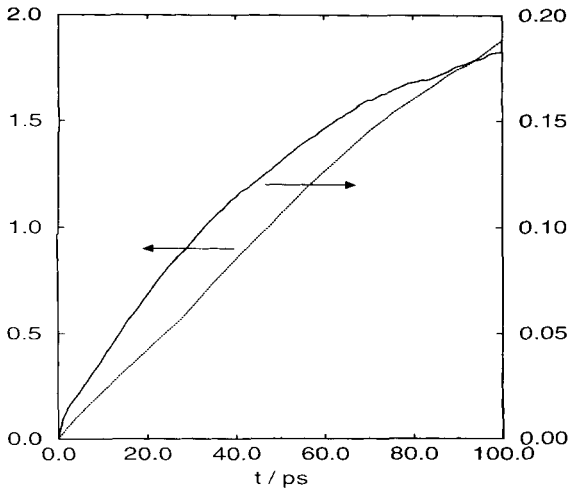

Fig. 5. Mean-square displacements (in nm^2) of a single water molecule as a function of time. The bulk water molecule (dotted line, left ordinate) reaches the diffusional regime within 1 ps; the first-shell water (continuous line, right ordinate), not within 100 ps.

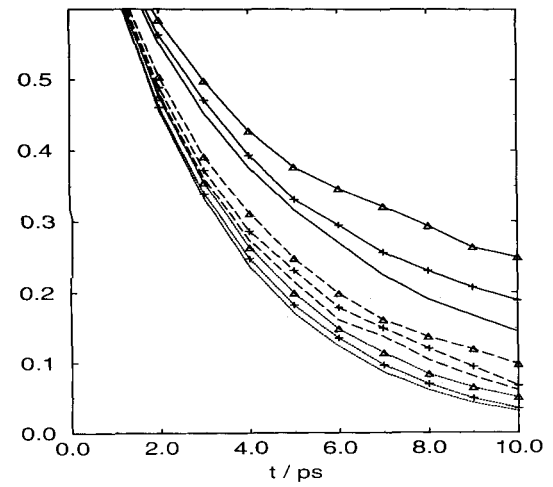

Fig. 6. Influence of protein on water reorientation (first Legendre polynomial P_1, 300 K). Line style indicates hydration shell number (continuous line, first shell; dashed line, second shell; dotted line, bulk); symbols indicate molecule-fixed vector (no symbol, HH vector; +, OH bond vector; triangles, dipole moment $\vec{\mu}$). The strong damping effect of the protein on the first-shell waters is obvious. The dipole moment displays slower reorientation than the OH and the HH vectors.

tions of pure water:[26,44–46] a rapid initial decay on a subpicosecond time scale with a librational mode is followed by a monotonous decay on a significantly slower time scale. For the extraction of correlation times from the single-particle correlation data, least-squares fits were done. The time interval used for the fits was chosen as one third of the shell residence time of the molecule considered. The target function used allows for two time scales: one accounts for the spatially restricted motion responsible for the initial decay, and the other for the slower motion of interest here:

$$g_{SM}(t) = (S^2 + (1 - S^2)e^{-t/\tau_f})e^{-t/\tau_s}. \quad (11)$$

S^2 is the intermediate plateau value reached on the fast time scale characterized by τ_f. The τ_f are typically in the subpicosecond range. Probability distributions for τ_s have been determined (Fig. 9). Considering the distributions for the first shell and the bulk, a common feature is revealed. Both are long-tail distributions with a peak below τ_s = 10 ps for the unperturbed relaxation. Longer relaxation times occur with decreasing probability. This decay takes place considerably more slowly for the first hydration shell. In other words, the distribution of single-molecule correlation times is broader for the first shell.

The distribution $P(\tau_s)$ of the τ_s relaxation times gives rise to a stretched exponential for the shell average:

$$\exp(-(t/\tau_K)^\beta) = \int_0^\infty d\tau_s P(\tau_s)\exp(-t/\tau_s). \quad (12)$$

In the following we consider the case $\beta = 0.5$, which has been found for the first shell. Substituting τ_s^{-1} by s, the above expression turns into a Laplace transformation:

$$\exp(-(t/\tau_K)^{1/2}) = \int_0^\infty ds\cdot\exp(-ts)s^{-2}P(s^{-1}). \quad (13)$$

Thus, $\exp(-(t/\tau_K)^{1/2})$ is the Laplace transform of $s^{-2}P(s^{-1})$. $s^{-2}P(s^{-1})$ is therefore given by[47]

$$s^{-2}P(s^{-1}) = (1/2)(\pi\cdot\tau_K)^{-1/2}\cdot s^{-3/2}\exp(-1/4\tau_K s). \quad (14)$$

Substituting s again by τ_s^{-1} one obtains

$$P(\tau_s) = (1/2)(\pi\cdot\tau_K)^{-1/2}\cdot\tau_s^{-1/2}\cdot\exp(-\tau_s/4\tau_K). \quad (15)$$

In the next step this theoretically derived distribution is compared to the simulated one. Figure 10 shows the τ_s distribution obtained from the single-molecule P_2^{HH} correlation functions (Fig. 9a) fitted to a target function of the type given in Eq. 15. This analytical form is very well apt to describe the distribution, although a larger value is found for the τ_K parameter of the distribution (3.88 ps) than for τ_K directly obtained from the shell-averaged correlation function (τ_K = 1.46 ps). This deviation may result from the fact that the real distribution displays a peak around 4 ps, whereas the theoretical model is monotonous throughout. Other analytical forms, e.g., a simple exponent, do not model the distribution as well as equation 15.

If reorientation is hindered by the environment, a stretched exponential time behavior will occur. With increasing perturbation, the KWW exponent β decreases. Classifying the influence of the environ-

TABLE II. Least-Squares Fit of Shell-Averaged Reorientational Correlation Functions to KWW Target Function $g(t) = \exp(-(t/\tau_\kappa)^\beta)$*

a. Data for 273 K

	P_1			P_2		
Vector	First shell	Second shell	Bulk	First shell	Second shell	Bulk
HH	8.65, 0.68	5.40, 0.78	4.82, 0.86	3.32, 0.49	2.06, 0.63	1.93, 0.70
OH	9.34, 0.65	5.65, 0.76	4.86, 0.85	2.83, 0.51	1.85, 0.62	1.70, 0.69
μ	12.58, 0.56	6.29, 0.70	4.99, 0.84	2.42, 0.47	1.57, 0.59	1.44, 0.66

b. Data for 300 K

	P_1			P_2		
Vector	First shell	Second shell	Bulk	First shell	Second shell	Bulk
HH	4.06, 0.71	2.87, 0.82	2.66, 0.88	1.46, 0.52	1.13, 0.68	1.08, 0.73
OH	4.53, 0.65	3.01, 0.79	2.66, 0.87	1.37, 0.52	1.05, 0.70	0.97, 0.74
μ	5.58, 0.58	3.23, 0.74	2.80, 0.84	1.12, 0.49	0.87, 0.64	0.85, 0.72

c. Data for 350 K

	P_1			P_2		
Vector	First shell	Second shell	Bulk	First shell	Second shell	Bulk
HH	1.71, 0.69	1.29, 0.83	1.23, 0.87	0.58, 0.51	0.50, 0.69	0.49, 0.72
OH	1.87, 0.63	1.33, 0.81	1.27, 0.84	0.55, 0.54	0.46, 0.70	0.46, 0.74
μ	2.30, 0.52	1.44, 0.76	1.33, 0.83	0.45, 0.49	0.39, 0.66	0.40, 0.71

*Each entry consists of two values, i.e., the correlation time τ_κ in picoseconds and the KWW exponent β.

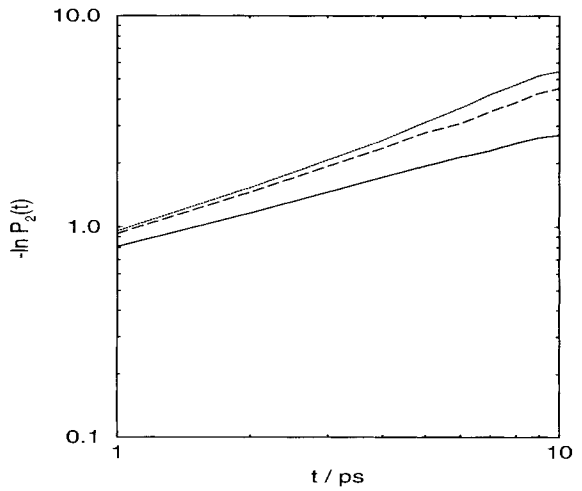

Fig. 7. Fractal time behavior of shell-averaged water reorientation shown for the second Legendre polynomial $P_2^{HH}(t)$ at 300 K. In a bilogarithmic plot of $-\ln P_2(t)$ vs. t, the exponent β of the Kohlrausch-Williams-Watts (KWW) function occurs as the slope. Continuous line, first shell; dashed line, second shell; dotted line, bulk.

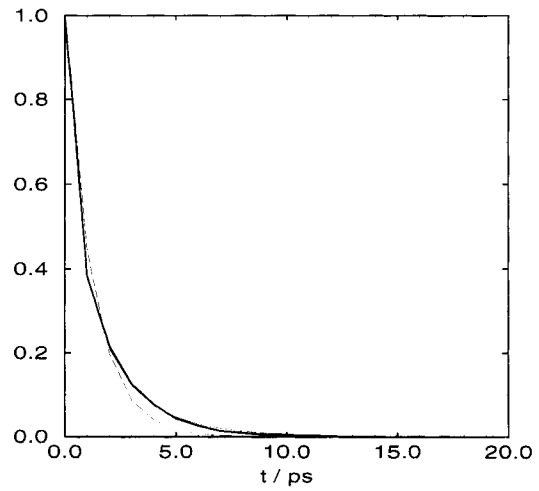

Fig. 8. Comparison of single exponential Debye model $g(t) = \exp(-t/\tau_D)$ (dashed line) and KWW model $g(t) = \exp(-(t/\tau_\kappa)^\beta)$ (thin continuous line) of bulk water reorientation (P_2^{HH}(300 K), thick continuous line). $\tau_D = 1.23$ ps, $\tau_\kappa = 1.08$ ps, $\beta = 0.73$. The mean squared error is 20×10^{-5} for the Debye model and 0.57×10^{-5} for the KWW model.

ment on the reorientational behavior of the various molecule-fixed vectors, the lowest values of β are always observed for the reorientation of the molecular dipole moment $\vec{\mu}$ (cf. Table II). As stated previously, this may be attributed to the fact that the dipole moment is subject to electrostatic forces which interfere with reorientation, whereas the interproton vector is affected to a lesser extent.

Lifetimes of neighborhood relations

The residence correlation function is the autocorrelation function of the Boolean variable χ which is either 1 or 0, depending on the water molecule being member of the shell considered or not (cf. Methods). Figure 11 shows the shell-averaged residence correlation functions for the first and second shells at 300 K.

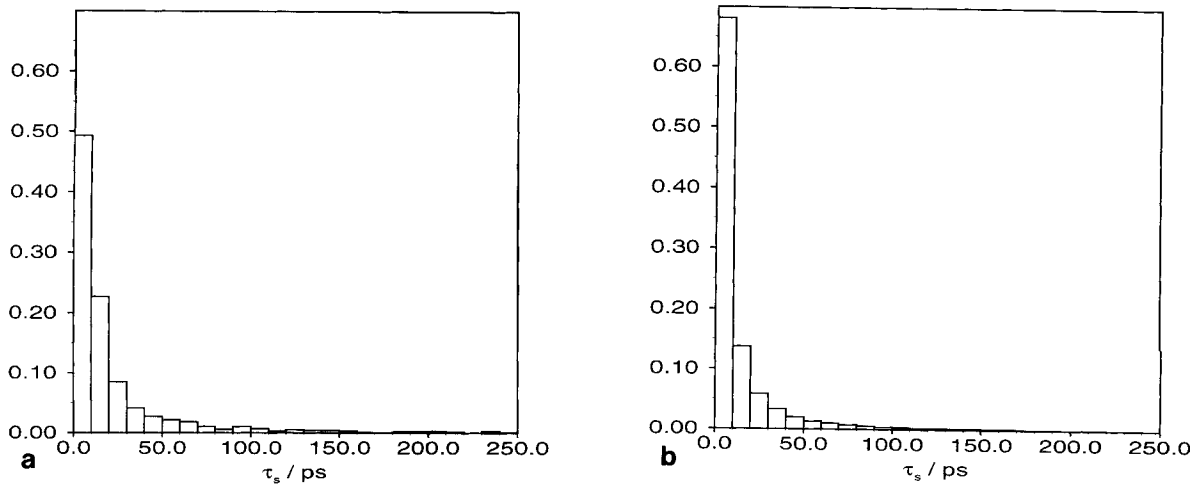

Fig. 9. Normalized probability distributions for the τ_s relaxation times of the single-molecule Legendre polynomials $P_2^{HH}(t)$ at 300 K. Data are for the reorientation of the intramolecular proton-proton vector. **a:** First hydration shell. **b:** Bulk fraction.

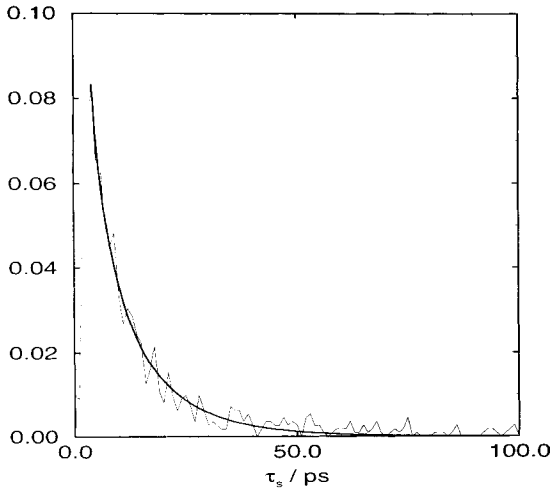

Fig. 10. Distribution of single molecule P_2^{HH} relaxation times τ_s (thin continuous line) modeled by function of the form $P(\tau_s) = a_0 \cdot \tau_s^{-1/2} \cdot \exp(-a_1\tau_s)$ (thick continuous line). The initial rise (dashed line) of the real distribution has been skipped before performing the least-squares fit.

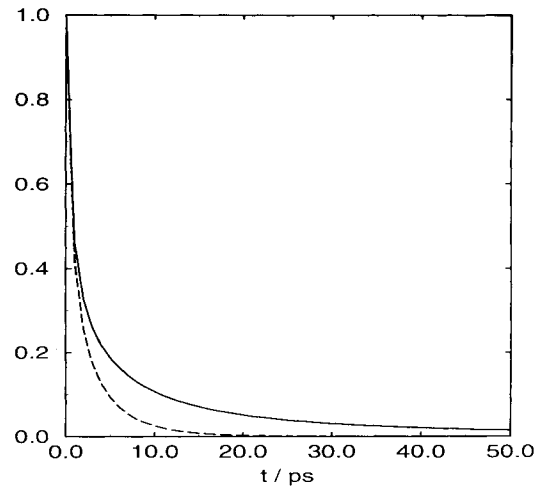

Fig. 11. Residence correlation function of the first (continuous line) and second (dashed line) hydration shells at 300 K. These functions behave similarly to the corresponding second-order orientational correlation functions.

The shell-averaged residence correlation functions decay on a time scale very similar to that of the shell-averaged second-order orientational autocorrelation functions ($P_2(t)$). They do not have simple exponential characteristics, but instead are well-described by a KWW function. The KWW exponent β is lower for the first shell (τ_κ = 1.562 psec, β = 0.426) than for the second shell (τ_κ = 1.234 psec, β = 0.621). This behavior is completely in parallel to the orientational autocorrelation functions.

The residence time distributions, i.e., the probability distributions of the residence times of single water molecules within a hydration shell, are shown in Figure 12. The curves for the first and second shell are very similar, but differ with regard to the linear average of residence times, which is 9.9 ps for the first shell and 3.8 ps for the second shell. This is due to the long tail of the residence time distribution of the first shell. Furthermore, the first shell contains a small fraction of water with very low mobility. There are 21 water molecules that appear as members of the first shell in each of the 1 ps-spaced coordinate frames of the 750-ps trajectory at 300 K. For the second solvation shell no permanent waters were observed. Residence times within the second shell do not transcend 50 ps.

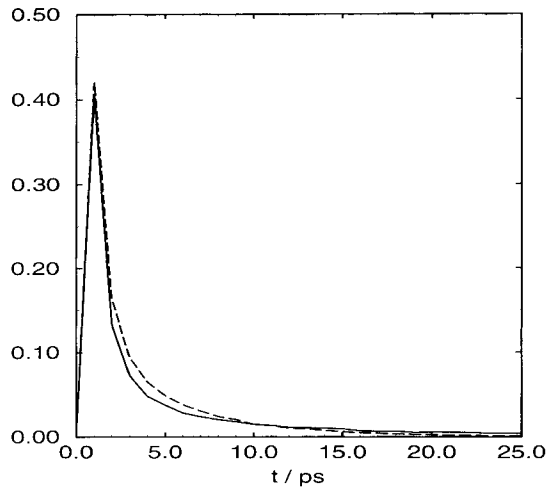

Fig. 12. Residence time distribution functions for the first (continuous line) and second (dashed line) shells. Resolution is 1 psec.

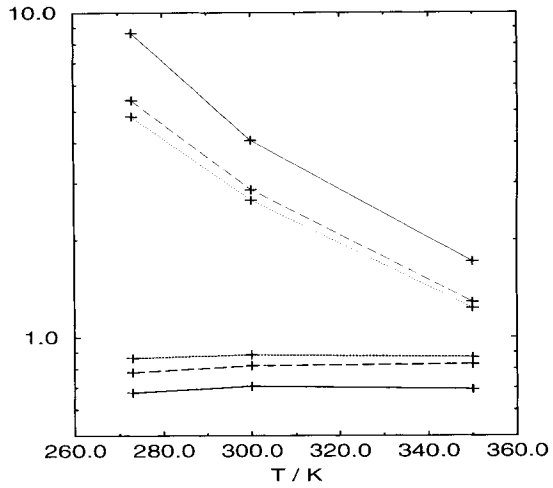

Fig. 13. Temperature dependence of Kohlrausch-Williams-Watts parameters τ_κ (in ps) and β. Simulations at 273, 300, and 350 K were performed. Data shown here are for the first Legendre polynomial of the intramolecular proton-proton vector P_1^{HH}. Parameters for the first shell (continuous lines), second shell (dashed lines), and bulk (dotted lines) are given. τ_κ, thin lines; β, thick lines.

Temperature Dependence of Fractal Time Behavior

The shell-averaged orientational autocorrelation functions were determined at 273, 300, and 350 K. Data are given in Table II. For all temperatures, time behavior is well described by KWW functions. Reorientation exhibits, as expected, a strong temperature dependence. Closer inspection of the KWW parameters τ_κ and β reveals that the temperature dependence is fully accounted for by the KWW correlation time τ_κ, whereas β remains essentially constant (Fig. 13). Especially from 300–350 K, β hardly changes. This finding indicates that the functional form of the distribution of single-molecule correlation times, which was derived explicitly for the case $\beta = 0.50$ (Eq. 15), does not change with temperature. What happens is a rescaling of the distribution P that accounts for the changes in τ_κ. This can be seen directly in Eq. 15: τ_κ appears as a parameter in P.

The differences between the hydration shells with regard to τ_κ decrease with rising temperature (Table III). A similar behavior of the rotational correlation times determined from deuteron relaxation measurements was observed for solutions of xenon.[7]

TABLE III. KWW Correlation Times τ_κ of Shell-Averaged First Legendre Polynomial of Intramolecular Proton-Proton Vector as a Function of Temperature*

T/K	First shell	Second shell	Bulk
273	1.79	1.12	1.00
300	1.53	1.08	1.00
350	1.39	1.05	1.00

*Data are normalized by bulk correlation time at respective temperature. Deviation of first and second shells from bulk behavior decreases with rising temperature.

DISCUSSION

A nascent polypeptide chain is "born" into an aqueous environment, and globular proteins usually remain there for their lifetime. Biological macromolecules exert a significant influence on small molecules in their vicinity. The most abundant small molecule is undoubtedly water. Pure water is a strongly interacting liquid. Thus, local structure relaxation, e.g., rotation of a single molecule, is tightly coupled to the environment. Close to a protein, this environment becomes much more complex owing to the diversity of surface sites. The fraction of water most perturbed by the protein is the first hydration shell. The definition of a hydration shell is always arbitrary to a certain extent. The Voronoi method employed in this study is characterized by its dependence on the instantaneous configuration of the solvent. Alternatively, cutoff radii derived from protein atom–water oxygen pair distribution functions may be used.[12] In this case a single configuration is treated with an ensemble-or. time-averaged criterion, respectively. Both methods, i.e., Voronoi polyhedra and cutoff radii, yield hydration levels h (g water/g protein) >1.0 for the first shell.

The present study focuses on the dynamic behavior of water under the influence of the small globular protein ubiquitin. Both translation and rotation were investigated. Translational motion of a bulk water molecule assumes diffusional characteristics within a picosecond. This is not the case for a first-shell water molecule. If one imagines a first-shell water molecule traveling along the protein surface,

it will encounter locally changing environments that impose different rates on its motion. Thus, the diffusional regime is reached (if at all) on much greater time scales. This change in characteristics of motion is accompanied by an overall retardation effect. The average diffusion coefficient of the first shell obtained from the simulation is compatible with the finding that surface waters generally give rise to positive NOEs with protons on the protein surface. Instead of following a single molecule on its way for its whole lifetime within a shell, the average translational mobility of water within a local environment can be analyzed. This has been done by Lounnas et al.[11] If the overall motion of the protein is negligible, a point on a grid can be regarded as a "site" within a relatively constant environment.

The heterogeneity of the protein surface affects water reorientation as well. The characteristics of the shell-averaged orientational correlation functions are shifted towards a Kohlrausch-Williams-Watts (KWW) time behavior. A KWW function involves two parameters: a correlation time τ_κ and an exponent β. For the first shell a dependence of the second Legendre polynomial on the square root of time is found, i.e., $\beta = 0.5$. Neumann et al.[36] reported a similar behavior for a very simple system, i.e., a spherical solute particle with a large dipole moment surrounded by Stockmayer particles. A stretched exponential time law is a feature of "glassy" relaxation in systems with strong interactions.[23,24] Relaxation is hindered in such a way that a single relaxation rate is no longer observed. The loss of a characteristic single-molecule correlation time is due to the influence of complex relaxation processes of the environment. Comparing the first hydration shell and the bulk, we observe a broadening of the distribution of single-molecule correlation times in the vicinity of the protein. A theoretical derivation of a distribution for the case $\beta = 0.5$ yields a function type that perfectly fits the distribution directly obtained from the simulation. Thus, a consistent picture of the "glassy" water structure in the vicinity of the protein is obtained.

The reorientations of the molecular dipole moment and of the interproton vector follow different characteristics. The KWW exponent β assumes lower values for dipole reorientation than for interproton vector reorientation in all shells and at all temperatures. This indicates that the dipole is subject to stronger interaction with the environment. In configurations where the dipole motion is spatially restricted owing to binding to other polar or charged species, on average the interproton vector is still more mobile.

The temperature dependence of reorientation is characterized by a varying correlation time τ_κ but an essentially constant KWW exponent β. Each of the molecule-fixed vectors considered, i.e., dipole moment, interproton vector, and OH bond vector, and each shell, have their characteristic β values which display negligible temperature dependence between 273–350 K. Thus, the time scale of rotation changes significantly, but the extent of coupling with the environment, which is high for the first shell and low for the bulk, remains the same. In other words, the functional form of the distributions of single-molecule correlation times is temperature-insensitive. The distributions are subject to rescaling upon temperature changes, but they retain their characteristics. The differences between the first shell, the second shell, and the bulk with regard to the correlation time τ_κ become smaller at higher temperatures.

Similar values of single-molecule orientational correlation times and average residence times of hydration sites have been reported.[48] The present study reveals a very similar time behavior of the shell-averaged orientational correlation functions and of the shell-averaged residence correlation functions. Although these findings are not fully comparable, they both indicate that on average there is a correlation between reorientation and lifetimes of neighborhood relations. This has been attributed to the fact that the breaking of hydrogen bonds is the key event in both reorientation and exchange processes in hydration shells.[48]

As stated above, the average number of first-shell water molecules is equivalent to a hydration level $h = 1.15$. Experimental methods are capable of detecting subsets of water with differing properties within the first shell. The amount of nonfreezable water in protein solutions is below $h = 0.40$.[8,9] The specific heat as a function of h reaches the asymptotic value characteristic of dilute solution in the range of $h < 0.4$, and water sorption isotherms display hysteresis, which is a consequence of the removal of the most tightly-bound water molecules, below $h = 0.3$.[9] Thus, a subset of the water forming the monolayer coverage of a protein is subject to a stronger perturbation of its behavior than the rest. It has been speculated that this might be water near polar surface groups.[49] Molecular dynamics simulations[10,12,14,50,51] have attempted to identify differences in water dynamics near polar, charged, and nonpolar surface groups. In part there is agreement among the respective results, but there are also contradictory findings. Komeiji et al.[51] investigated translational diffusion in the vicinity of the *trp*-holorepressor and found no significant difference between water molecules solvating different atom types. Lee and Rossky[14] studied polar and apolar model surfaces and found slower reorientation near polar than near apolar surfaces. Translational diffusion perpendicular to the surface is retarded for both types of surfaces, but to a greater extent near polar surfaces. Using the argument of Lounnas and Pettitt[48] and assuming a correlation between reorientation and residence times, the findings of Lee and Rossky[14] are supported by the studies

of Brunne et al.[12] on BPTI. Brunne et al.[12] found shorter residence times for waters near nonpolar atoms than near polar atoms, but shortest for waters near charged atoms. The latter finding is contradicted by Muegge and Knapp[10] and Garcia and Stiller,[50] who found the following order of residence times τ: $\tau_{charged} > \tau_{polar} > \tau_{nonpolar}$. Generally, simulated residence times are shorter than those estimated from NMR spectroscopy.[6] It is not clear if this stems from uncertainties in the NMR data or from artifacts in the simulations. Altogether, there is still space for improvement. First, all the above-mentioned simulation studies used a spherical cutoff for truncation of long-range electrostatic interactions. It has been demonstrated that this procedure may introduce artifacts into the dynamical behavior of the simulated system.[52,53] Therefore, the present study employed the Ewald method for the calculation of the Coulomb interaction. Secondly, the description of the protein–water interactions may need an optimization. This argument has been raised as an explanation for the fact that overall rotation of peptides and proteins is too fast in simulation by a factor of 3.[54,55] Improvement may involve a fine-tuning of the interaction function parameters and refined interaction paradigms, e.g., polarizability of solvent and solute. Van Belle and Wodak[56] have found that a polarizable water model (PSPC)[57] displays a less pronounced retardation effect than SPC water in the vicinity of nonpolar solutes. And finally, the residence times extracted from simulations depend strongly on how often residences are checked, as has been pointed out.[10] Summing up, we may say that a reassessment of the subtle local differences in the protein-solvent interface with refined tools is desirable.

ACKNOWLEDGMENTS

This work was supported by the Austrian "Fonds zur Förderung der wissenschaftlichen Forschung project number P10095-CHE. The authors thank Martin Neumann for stimulating discussions concerning this subject.

REFERENCES

1. Karplus, P.A., Faerman, C. Ordered water in macromolecular structure. Curr. Opin. Struct. Biol. 4:770–776, 1994.
2. Levitt, M., Park, B.H. Water: Now you see it, now you don't. Structure 1:223–226, 1993.
3. Teeter, M.M. Water-protein interactions: Theory and experiment. Annu. Rev. Biophys. Biophys. Chem. 20:577–600, 1991.
4. Levitt, M., Sharon, R. Accurate simulation of protein dynamics in solution. Proc. Natl. Acad. Sci. U.S.A. 85:7557–7561, 1988.
5. Daggett, V., Levitt, M. Realistic simulations of native-protein dynamics in solution and beyond. Annu. Rev. Biophys. Biomol. Struct. 22:353–380, 1993.
6. Otting, G., Liepinsh, E., Wüthrich, K. Protein hydration in aqueous solution. Science 254:974–980, 1991.
7. Haselmeier, R., Holz, M., Marbach, W., Weingärtner, H. Water dynamics near a dissolved noble gas. First direct experimental evidence for a retardation effect. J. Phys. Chem. 99:2243–2246, 1995.
8. Miura, N., Hayashi, Y., Shinyashiki, N., Mashimo, S. Observation of unfreezable water in aqueous solution of globule protein by microwave dielectric measurement. Biopolymers 36:9–16, 1995.
9. Gregory, R.B. "Protein-Solvent Interactions." New York: Marcel Dekker, 1995.
10. Muegge, I., Knapp, E.W. Residence times and lateral diffusion of water at protein surfaces: Application to BPTI. J. Phys. Chem. 99:1371–1374, 1995.
11. Lounnas, V., Pettitt, M., Phillips, G.N., Jr. A global model of the protein-solvent interface. Biophys. J. 66:601–614, 1994.
12. Brunne, R.M., Liepinsh, E., Otting, G., Wüthrich, K., van Gunsteren, W.F. Hydration of Proteins. J. Mol. Biol. 231: 1040–1048, 1993.
13. Steinbach, P.J., Brooks, B.R. Protein hydration elucidated by molecular dynamics simulation. Proc. Natl. Acad. Sci. U.S.A. 90:9135–9139, 1993.
14. Lee, S.H., Rossky, P.J. A comparison of the structure and dynamics of liquid water at hydrophobic and hydrophilic surfaces—A molecular dynamics simulation study. J. Chem. Phys. 100:3334–3345, 1994.
15. Gerstein, M., Lynden-Bell, R.M. What is the natural boundary of a protein in solution? J. Mol. Biol. 230:641–650, 1993.
16. Phillips, G.N., Pettitt, M. Structure and dynamics of the water around myoglobin. Protein Sci 4:149–158, 1995.
17. Lounnas, V., Pettitt, M., Findsen, L., Subramaniam, S. A microscopic view of protein solvation. J. Phys. Chem. 96: 7157–7159, 1992.
18. Kuhn, L.A., Siani, M.A., Pique, M.E., Fisher, C.L., Getzoff, E.D., Tainer, J.A. The interdependence of protein surface topography and bound water molecules revealed by surface accessibility and fractal density measures. J. Mol. Biol. 228:13–22, 1992.
19. Vijay-Kumar, S., Bugg, C.E., Cook, W.J. Structure *of ubi*quitin refined at 1.8 Å resolution. J. Mol. Biol., 194:531–544, 1987.
20. Voronoi, G.F. Nouvelles applications des paramètres continus à la théorie des formes quadratiques. J. Reine Angew. Math. 134:198–287, 1908.
21. Richards, F.M. Areas, volumes, packing, and protein structure. Annu. Rev. Biophys. Bioeng. 6:151–176, 1977.
22. Denisov, V.P., Halle, B. Dynamics of the internal and external hydration of globular proteins. J. Am. Chem. Soc. 116:10324–10325, 1994.
23. Ngai, K.L., Rendell, R.W., Rajagopal, A.K., Teitler, S. Three coupled relations for relaxations in complex systems. Ann. N.Y. Acad. Sci. 484:150–184, 1986.
24. Shlesinger, M.F. Fractal time in condensed matter. Annu. Rev. Phys. Chem. 39:269–290, 1988.
25. Berendsen, H.J.C., Postma, J.P.M., van Gunsteren, W.F., Hermans, J. "Intermolecular Forces." Dordrecht: Reidel, 1981.
26. Postma, J.P.M. "A Molecular Dynamics Study of Water." Ph.D. thesis, Rijksuniversiteit Groningen, 1985.
27. Van Gunsteren, W.F., Berendsen, H.J.C. "GROningen MOlecular Simulation (GROMOS) Library Manual." Groningen, The Netherlands: Biomos, 1987.
28. Ewald, P.P. Die Berechnung optischer und elektrostatischer Gitterpotentiale. Ann. Phys. 64:253–287, 1921.
29. De Leeuw, S.W., Perram, J.W., Smith, E.R. Simulation of electrostatic systems in periodic boundary conditions. I. Lattice sums and dielectric constants. Proc. R. Soc. Lond. [A] 373:27–56, 1980.
30. Adams, D.J., Dubey, G.S. Taming the Ewald sum in the computer simulation of charged systems. J. Comput. Phys., 72:156–176, 1987.
31. Van Gunsteren, W.F., Berendsen, H.J.C. Algorithms for macromolecular dynamics and constraint dynamics. Mol. Phys. 34:1311–1327, 1977.
32. Berendsen, H.J.C., Postma, J.P.M., DiNola, A., Haak, J.R. Molecular dynamics with coupling to an external bath. J. Chem. Phys. 81:3684–3690, 1984.
33. Kell, G.S. Thermodynamic and Transport Properties of Liquid Water. Franks, F. (ed.). "Water. A Comprehensive Treatise," vol. 1. New York: Plenum Press, 1972.
34. Bernal, J.D., King, S.V. "Physics of Simple Liquids." Amsterdam: North Holland, 1968.
35. Gerstein, M., Tsai, J., Levitt, M. The volume of atoms on

the protein surface: Calculated from simulation, using Voronoi polyhedra. J. Mol. Biol. 249:955–966, 1995.
36. Neumann, M., Vesely, F.J., Steinhauser, O., Schuster, P. Solvation of large dipoles. A molecular dynamics study II. Mol. Phys. 37:1725–1743, 1979.
37. Gerstein, M., Lynden-Bell, R.M. Simulation of water around a model protein helix. 1. Two-dimensional projections of solvent structure. J. Phys. Chem. 97:2982–2990, 1993.
38. Hubbard, S.J., Thornton, J.M. NACCESS. Computer Program. Technical report, Department of Biochemistry and Molecular Biology, University College London, 1993.
39. Kohlrausch, R. Ann. Phys. "Über das Dellmann'sche Elektrometer." (Leipzig) 12:353, 1847.
40. Williams, G. Watts, D.C. Trans. "Non-symmetrical dielectric relaxation behavior arising from a simple empirical decay function." Faraday Soc. 66:80, 1970.
41. Press, W.H., Flannery, B.P., Teukolsky, S.A., Vetterling, W.T. "Numerical Recipes. The Art of Scientific Computing." Cambridge and New York: Cambridge University Press, 1986.
42. Palmer, R.G., Stein, D.L., Abrahams, E., Anderson, P.W. Models of hierarchically constrained dynamics for glassy relaxation. Phys. Rev. Lett. 53:958–961, 1984.
43. Neumann, M. Struktur und Dynamik von Solvathüllen um hochpolare Moleküle: Eine Molekulardynamik-Prinzipstudie. Ph.D. thesis, Universität Wien, 1978.
44. Frattini, R., Ricci, M.A., Ruocco, G., Sampoli, M. Temperature evolution of single particle correlation functions of liquid water. J. Chem. Phys. 92:2540–2547, 1990.
45. Stillinger, F.H., Rahman, A. Molecular dynamics study of temperature effects on water structure and kinetics. J. Chem. Phys. 57:1281–1292, 1972.
46. Rahman, A., Stillinger, F.H. Molecular dynamics study of liquid water. J. Chem. Phys. 55:3336–3359, 1971.
47. Rottmann, K. "Mathematische Formelsammlung." Bibliographisches Institut, Mannheim, 1984.
48. Lounnas, V., Pettitt, B.M. Distribution function implied dynamics versus residence times and correlations: Solvation shells of myoglobin. Proteins 18:148–160, 1994.
49. Finney, J.L., Poole, P.L. "Protein hydration and enzyme activity: The role of hydration-induced conformation and dynamic changes in the activity of lysozyme." Comments Mol. Cell. Biophys. 2:129–151, 1984.
50. Garcia, A.E., Stiller, L. Computation of the mean residence time of water in the hydration shells of biomolecules. J. Comput. Chem. 14:1396–1406, 1993.
51. Komeiji, Y., Uebayasi, M., Someya, J., Yamato, I. A molecular dynamics study of solvent behavior around a protein. Proteins 16:268–277, 1993.
52. Schreiber, H., Steinhauser, O. Cutoff size does strongly influence molecular dynamics results on solvated polypeptides. Biochemistry 31:5856–5860, 1992.
53. Schreiber, H., Steinhauser, O. Taming cut-off induced artifacts in molecular dynamics studies of solvated polypeptides. J. Mol. Biol. 228:909–923, 1992.
54. Brüschweiler, R., Roux, B., Blackledge, M., Griesinger, C., Karplus, M., Ernst, R.R. Influence of rapid intramolecular motion on NMR cross-relaxation rates. A molecular dynamics study of antamanide in solution. J. Am. Chem. Soc. 114:2289–2302, 1992.
55. Smith, P.E., van Gunsteren, W.F. Translational and rotational diffusion of proteins. J. Mol. Biol. 236:629–636, 1994.
56. Van Belle, D., Wodak, S.J. Molecular dynamics study of methane hydration and methane association in a polarizable water phase. J. Am. Chem. Soc. 115:647–652, 1993.
57. Ahlström, P., Wallqvist, A., Engström, S., Jönsson, B. A molecular dynamics study of polarizable water. Mol. Phys. 68:563–581, 1989.